

Di-photon production at the LHC

Zvi Bern^a, Lance Dixon^b, and Carl Schmidt^c (presenter)

^a*Department of Physics and Astronomy, UCLA, Los Angeles, CA 90095-1547, USA*

^b*Stanford Linear Accelerator Center, Stanford University, Stanford, CA 94309, USA*

^c*Department of Physics and Astronomy, Michigan State University, East Lansing, MI 48824, USA*

The standard model production of two photons is one of the most important backgrounds to light Higgs boson production at the LHC. In this talk we discuss the di-photon background, with emphasis on the effects of the recently calculated next-to-leading-order (NLO) corrections to the gluon-gluon-initiated component. We find that the K -factor for this component is smaller than that for the analogous $gg \rightarrow H$ process, and that the correction to the total irreducible di-photon production is modest. We also investigate ways to enhance the statistical significance of the Higgs signal in the $\gamma\gamma$ channel.

1 Introduction

One of the primary goals of the LHC is to provide clues to the nature of electroweak symmetry breaking. In the standard model this symmetry breaking is provided by the condensation of a fundamental weak scalar doublet, which leaves behind a single neutral scalar, the Higgs boson, as residue. This standard model Higgs boson is constrained by precision electroweak measurements to have $m_H \lesssim 196\text{--}230$ GeV at 95% CL.¹ A light neutral scalar boson with similar properties is also often predicted in extensions of the standard model; for example, in the Minimal Supersymmetric Standard Model (MSSM) the lightest Higgs boson is predicted to have a mass below about 135 GeV.²

For $m_H < 140$ GeV, the most promising discovery mode for the Higgs boson at the LHC involves production via gluon fusion, $gg \rightarrow H$, followed by the rare decay into two photons, $H \rightarrow \gamma\gamma$.³ Although this mode has a very large continuum $\gamma\gamma$ background,⁴ the excellent mass resolution of the LHC detectors should allow the detection of the narrow Higgs resonance signal above the background.⁵ For optimizing this analysis, it is necessary to have the best theoretical understanding of both signal and background beforehand.

The perturbative contribution to $pp \rightarrow \gamma\gamma X$ proceeds at lowest order via the quark annihilation subprocess $q\bar{q} \rightarrow \gamma\gamma$. The NLO corrections to this process have been calculated,^{6,7} as have processes involving parton fragmentation to photons at NLO.⁷ The remaining important perturbative contribution is the gluon annihilation subprocess $gg \rightarrow \gamma\gamma$. Although this arises at order α_s^2 through a quark box loop, it is still of the same size as the quark annihilation subprocess, due to the large gluon luminosity at the LHC.^{4,8,6,7} All of these perturbative contributions have been included in the Monte Carlo program DIPHOX,⁷ with the direct and fragmentation contributions evaluated at NLO and the gluon box diagram evaluated at lowest order α_s^2 . In this talk we report on the impact of extending the gluon box contribution to NLO.⁹ (Note that we refer to this correction as NLO in comparison to the lowest-order gluon box contribution; in fact, it is N³LO compared to the order α_s^0 quark annihilation process.)

Before we discuss this correction and some phenomenological studies in the next sections, it is important to emphasize that our analysis only includes the irreducible di-photon background. There is also a very large reducible background, arising from photons which are faked by jets or hadrons, especially π^0 's. Although these reducible backgrounds can be suppressed greatly by photon isolation cuts,⁵ more detailed experimental studies of pion fragmentation at large momentum fraction in jets are necessary to accurately quantify the impact of this reducible background.¹⁰

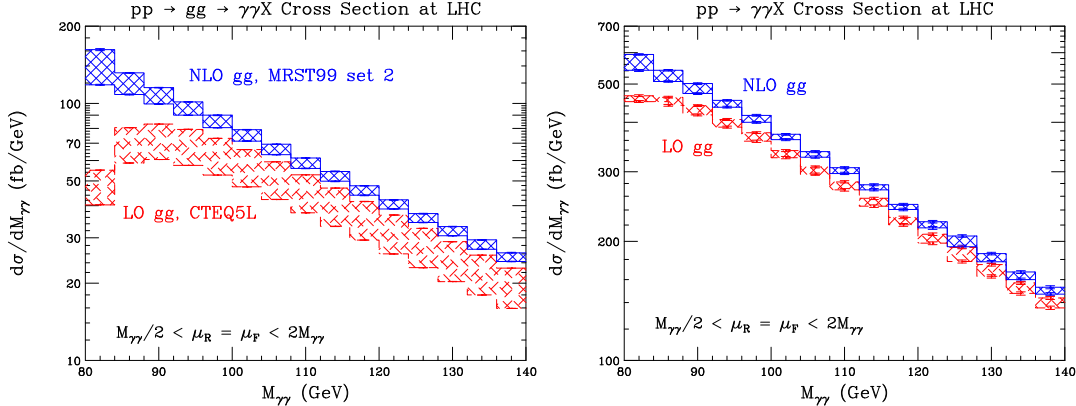


Figure 1: Scale dependence of (a) the gluon fusion subprocess contribution to $pp \rightarrow \gamma\gamma X$, and (b) the total $pp \rightarrow \gamma\gamma X$ production cross section, for standard photon isolation with $R = 0.4$, $E_{T \max} = 15$ GeV. In both plots, the bands represent the result of varying μ_R and μ_F together over region $0.5M_{\gamma\gamma} < \mu_R = \mu_F < 2M_{\gamma\gamma}$. The dashed (solid) hatched band corresponds to including the gluon fusion subprocess at LO (NLO). For the leading order band in (a) only, the LO CTEQ5L parton distributions¹⁴ were used; otherwise the NLO MRST99 set 2 distributions¹³ were employed.

2 Effect of gluon fusion at NLO

Although the gluon box contribution begins at one-loop and is order α_s^2 , the QCD corrections to it can be treated exactly as a NLO calculation,¹¹ independent from the other perturbative contributions at this order. We have implemented this NLO cross section in a Monte Carlo routine, which allows the imposition of general kinematic cuts. Details of this calculation can be found in our full journal article.⁹

For the phenomenological analyses, we impose the following cuts on the two photons: $p_T(\gamma_1) > 40$ GeV, $p_T(\gamma_2) > 25$ GeV, $|y(\gamma_{1,2})| < 2.5$. In addition, we impose one of two photon isolation criteria: *standard* cone isolation — the amount of transverse hadronic energy E_T in a cone of radius $R = \sqrt{(\Delta\eta)^2 + (\Delta\phi)^2}$ must be less than $E_{T \max}$; or *smooth* cone isolation¹² — the amount of transverse hadronic energy E_T in *all* cones of radius r with $r < R$ must be less than $E_{T \max}(r) \equiv p_T(\gamma) \epsilon (1 - \cos r) / (1 - \cos R)$, for some ϵ . The smooth cone isolation criterion is designed to remove all fragmentation contributions in an infrared-safe manner. For all calculations using this isolation criterion we implemented the NLO quark-fusion contributions, as well as the NLO gluon box contributions, directly in our Monte Carlo. For calculations using the standard cone isolation criterion we have used our own Monte Carlo to calculate the NLO gluon box contributions, and we have used DIPHOX⁷ to calculate all other contributions.

In fig. 1(a) we plot just the gluon box contribution at LO and NLO while varying the renormalization and factorization scales together over the range $0.5M_{\gamma\gamma} < \mu_R = \mu_F < 2M_{\gamma\gamma}$. As is typical of gluon-initiated processes, the NLO cross section is larger than at LO, and the scale-dependence is reduced. We note, however, that the reduction in scale-dependence is much less impressive if μ_R and μ_F are allowed to vary independently.⁹

It is useful to compare the NLO enhancement in the $gg \rightarrow \gamma\gamma X$ process with that of the $gg \rightarrow HX$ process by comparing K factors, defined as the ratio of the NLO and LO cross sections. Using the NLO MRST99 set 2 distributions¹³ for both the numerator and denominator with $\mu_R = \mu_F = 0.5M_{\gamma\gamma}$ and the same sets of cuts as in fig. 1(a) for $M_{\gamma\gamma} = 118$ GeV, we obtain $K_{gg \rightarrow \gamma\gamma} = 1.61$ and $K_{\text{Higgs}} = 2.54$. Thus, some earlier studies of the di-photon background, which adopted the K factor for Higgs production, overestimated this background. The larger K factor for Higgs production can be traced to two effects. The effective Hgg coupling, which results from the heavy top quark loop, receives a short-distance renormalization that has no counterpart in direct $\gamma\gamma$ production. In addition, the real correction to Higgs production has a

harder transverse momentum spectrum than direct $\gamma\gamma$ production, since the dominant scale in the loop is the top mass, rather than the parton momenta. Recently, the higher order coefficients that affect the K factor in the resummation of the di-photon cross section at small transverse momentum have been extracted from this NLO calculation.¹⁵

In fig. 1(b) we show the effects of computing the gluon fusion subprocess at NLO on the total irreducible di-photon background. The upper band contains all processes, including gluon fusion, quark annihilation, and fragmentation contributions at NLO, while the lower band contains gluon fusion at LO and the other processes at NLO. The scale variation and kinematic cuts are the same as for fig. 1(a). As before, the scale dependence is much greater for both bands if μ_R and μ_F are varied independently.⁹ For $M_{\gamma\gamma}$ greater than 100 GeV, the NLO gluon box correction to the total cross section is about 10% or less; therefore this subprocess can be considered to be under adequate theoretical control.

3 Di-photon background kinematics and Higgs Signal

Using our Monte Carlo, we have studied some kinematic properties of the di-photon production with the aim of increasing the statistical significance of the Higgs signal above background. For this study we have implemented the Higgs signal in the Monte Carlo at NLO in the heavy top mass limit, with subsequent decay to $\gamma\gamma$. We assumed a Higgs mass of 118 GeV, and we counted the number of events in a mass bin of 4 GeV for 30 fb⁻¹ of integrated luminosity. We also included an experimental efficiency factor of 0.57 for both signal and background (0.81 per γ for identification, 0.87 for fiducial cuts), and we included, as a rough estimate, a reducible background of 20% of the $\gamma\gamma$ continuum background.

One feature that distinguishes the Higgs signal from the irreducible background is the correlation between the photons and any accompanying hadronic radiation. Since the Higgs boson is a colorless object, its decay photons will be produced uncorrelated with hadronic radiation. On the other hand, a significant component of the background consists of $qg \rightarrow qg\gamma$, where the γ has a collinear enhancement when produced near the final-state quark. This suggests that one can suppress the background relative to the signal by increasing the severity of the isolation cut—either by increasing the cone size R , or decreasing ϵ or $E_{T\text{max}}$. As an example the statistical significance (S/\sqrt{B}) was increased by 7% by increasing R from 0.4 to 2, while keeping $E_{T\text{max}} = 15$ GeV fixed. Similar results were found for the smooth cone algorithm.

Unfortunately, an isolation cone as large as $R = 2$ may not be phenomenologically viable for both theoretical and experimental reasons. A more infrared-safe and experimentally better-behaved procedure is to veto on jets within a larger cone R_{jet} around the photons, in addition to an isolation cut with $R < R_{\text{jet}}$. The jet veto is more infrared-safe than a large isolation cone, because it only restricts hadronic energy within the jet cone, not the full jet veto region R_{jet} . It is also more viable experimentally, since one need not worry about loss of efficiency due to detector noise or nonperturbative sources of hadronic energy in the large isolation cone. We have investigated the use of a jet veto to enhance the statistical significance of the Higgs signal, but found the significance to be relatively insensitive to it. More study is needed to find the best way to utilize the hadronic energy distribution in the events to optimize the Higgs signal.

A second feature that distinguishes the signal and background is the angular distribution of the photons. The signal photons, coming from the decay of a scalar particle, are isotropic in the Higgs rest frame, whereas the background photons tend to be more peaked along the beam axes. This results in a distinctly different distribution in the di-photon rapidity difference, $y^* = (y(\gamma_1) - y(\gamma_2))/2$, for the signal and background events. This distribution is the most robust discriminator that we found, offering a modest ($\sim 4\%$) improvement in the statistical significance of the Higgs signal.

More details of this calculation and the analysis can be obtained in our full journal article.⁹

Further studies, which include reducible di-photon background contributions,¹⁰ additional NNLO contributions, and more detailed experimental simulations will greatly enhance our understanding of the di-photon background, leading to increased sensitivity for the Higgs search at the LHC, and potentially reducing the time required for the discovery of a light Higgs boson.

Acknowledgments

We thank Thomas Binoth for providing us with a copy of DIPH0X. The work of Z.B. and L.D. was supported by the US Department of Energy under contracts DE-FG03-91ER40662 and DE-AC03-76SF00515, respectively. The work of C.S. was supported by the US National Science Foundation under grant PHY-0070443.

References

1. G. Degrassi, arXiv:hep-ph/0102137; J. Erler, arXiv:hep-ph/0102143; D. Abbaneo *et al.* [ALEPH, DELPHI, L3 and OPAL Collaborations, LEP Electroweak Working Group, and SLD Heavy Flavor and Electroweak Groups], arXiv:hep-ex/0112021.
2. M. Carena *et al.*, Nucl. Phys. B **580**, 29 (2000); J.R. Espinosa and R. Zhang, Nucl. Phys. B **586**, 3 (2000); A. Brignole *et al.*, Nucl. Phys. B **631**, 195 (2002).
3. J.R. Ellis *et al.*, Nucl. Phys. B **106**, 292 (1976); M.A. Shifman *et al.*, Sov. J. Nucl. Phys. **30**, 711 (1979) [Yad. Fiz. **30**, 1368 (1979)]; J.F. Gunion *et al.*, Phys. Rev. D **34**, 101 (1986); J.F. Gunion, G.L. Kane and J. Wudka, Nucl. Phys. B **299**, 231 (1988).
4. R.K. Ellis, I. Hinchliffe, M. Soldate and J.J. van der Bij, Nucl. Phys. B **297**, 221 (1988).
5. ATLAS collaboration, “ATLAS detector and physics performance, technical design report,” vol. 2, report CERN/LHCC 99-15, ATLAS-TDR-15; CMS collaboration, “CMS: The electromagnetic calorimeter, technical design report,” report CERN/LHCC 97-33, CMS-TDR-4; V. Tisserand, “The Higgs to two photon decay in the ATLAS detector,” talk given at the VI International Conference on Calorimetry in High-Energy Physics, Frascati (Italy), June, 1996, LAL 96-92; Ph.D. thesis, LAL 97-01, February, 1997; M. Wielers, “Isolation of photons,” report ATL-PHYS-2002-004.
6. E.L. Berger *et al.*, Nucl. Phys. B **239**, 52 (1984); P. Aurenche *et al.*, Z. Phys. C **29**, 459 (1985); B. Bailey *et al.*, Phys. Rev. D **46**, 2018 (1992); B. Bailey and J.F. Owens, Phys. Rev. D **47**, 2735 (1993); B. Bailey and D. Graudenz, Phys. Rev. D **49**, 1486 (1994); C. Balazs *et al.*, Phys. Rev. D **57**, 6934 (1998); C. Balazs and C.-P. Yuan, Phys. Rev. D **59**, 114007 (1999) [Erratum-ibid. D **63**, 059902 (1999)]; T. Binoth *et al.*, Phys. Rev. D **63**, 114016 (2001); T. Binoth, arXiv:hep-ph/0005194.
7. T. Binoth *et al.*, Eur. Phys. J. C **16**, 311 (2000).
8. L. Ametller, E. Gava, N. Paver and D. Treleani, Phys. Rev. D **32**, 1699 (1985); D.A. Dicus and S.S.D. Willenbrock, Phys. Rev. D **37**, 1801 (1988).
9. Z. Bern, L. Dixon and C. Schmidt, Phys. Rev. D **66**, 074018 (2002).
10. T. Binoth, J.P. Guillet, E. Pilon and M. Werlen, arXiv:hep-ph/0203064.
11. Z. Bern, A. De Freitas and L.J. Dixon, JHEP **0109**, 037 (2001); Z. Bern, L. Dixon and D.A. Kosower, Phys. Rev. Lett. **70**, 2677 (1993); D. de Florian and Z. Kunszt, Phys. Lett. B **460**, 184 (1999); C. Balazs *et al.*, Phys. Lett. B **489**, 157 (2000).
12. S. Frixione, Phys. Lett. B **429**, 369 (1998).
13. A.D. Martin *et al.*, Eur. Phys. J. C **14**, 133 (2000).
14. H.L. Lai *et al.* [CTEQ Collaboration], Eur. Phys. J. C **12**, 375 (2000).
15. P. M. Nadolsky and C. R. Schmidt, Phys. Lett. B **558**, 63 (2003).